Journal of
Marine Science and Engineering

MDPI

Article

Numerical Study on Flexible Pipe End Fitting Progressive Failure Behavior Based on Cohesive Zone Model

Tao Zhang [1], Qingzhen Lu [2,3,*], Jun Yan [1,3], Shichao Wang [2], Qianjin Yue [2], Shanghua Wu [2], Hailong Lu [1] and Jinlong Chen [4]

[1] State Key Laboratory of Structural Analysis for Industrial Equipment, Department of Engineering Mechanics, Dalian University of Technology, Dalian 116024, China
[2] State Key Laboratory of Structural Analysis for Industrial Equipment, School of Ocean Science and Technology, Dalian University of Technology, Panjin 124221, China
[3] Ningbo Research Institute of Dalian University of Technology, Ningbo 315016, China
[4] Jiangsu Hengtong Marine Cable Systems Co., Ltd., Changshu 215537, China
* Correspondence: luqingzhen@dlut.edu.cn; Tel.: +86-158-4087-1402

Abstract: Flexible pipes are extensively used to connect seabed and floating production systems for the development of deep-water oil and gas. In the top connection area, end fitting (EF) is the connector between the flexible pipe and floating platform, as a critical component for structural failure. To address this issue, a combined numerical and experimental prediction method is proposed in this paper to investigate the failure behavior of flexible pipes EF considering tensile armor and epoxy resin debonding. In order to analyze the stress distribution of the tensile armor and the damage state of the bonding interface as the tensile load increases, a finite element model of the EF anchorage system is established based on the cohesive zone model (CZM). Additionally, the effects of the epoxy resin shear strength (ss) and the steel wire yield strength (ys) on the structural load-bearing capacity are discussed in detail. The results indicate that wire strength and interface bonding have a substantial effect on the anchorage system's failure behavior, and the low-strength wire anchorage system has a three-stage failure behavior with wire yielding as the predominant failure mode, while the high-strength wire anchorage system has a two-stage failure behavior with interface debonding as the predominant failure mode.

Keywords: flexible pipe; end fitting; progressive failure; cohesive zone model

Citation: Zhang, T.; Lu, Q.; Yan, J.; Wang, S.; Yue, Q.; Wu, S.; Lu, H.; Chen, J. Numerical Study on Flexible Pipe End Fitting Progressive Failure Behavior Based on Cohesive Zone Model. *J. Mar. Sci. Eng.* **2023**, *11*, 116. https://doi.org/10.3390/jmse11010116

Academic Editor: Cristiano Fragassa

Received: 26 November 2022
Revised: 17 December 2022
Accepted: 19 December 2022
Published: 5 January 2023

1. Introduction

Over the years, oil and gas development has extended further into deep water, and flexible pipes are widely used in the floating production system to connect the seabed infrastructure and the floating platform [1]. An unbonded flexible pipe is a typical composite multi-layer structure designed for a harsh environment, which includes a carcass, inner sheath, pressure armor, tensile armor, anti-wear tapes, and outer sheath, and the structure of typical unbonded flexible pipes is described in detail in the API 17 B [2] specification (as is shown in Figure 1); the polymeric layers act as seals, insulator, and/or anti-wear elements, while the metallic layers bear the most mechanical load [3]. During service, flexible pipes are subject to various loads, including tension, bending, and internal and external pressure. During ultra-deep-water operations, the top connection area is subjected to high tensile loads caused by the pipe's self-weight, causing a significant risk to the safety of the flexible pipe. End fitting (EF) is one of the most crucial auxiliary devices of flexible pipe systems. As flexible pipes are utilized in deeper and deeper water, the issue of the end fitting's ultimate load-bearing capacity becomes increasingly significant. EF also serves as a termination for the pipe's primary structural components, i.e., the carcass, internal polymer sheath (fluid barrier), pressure armor, tensile armor, and external polymer sheath.

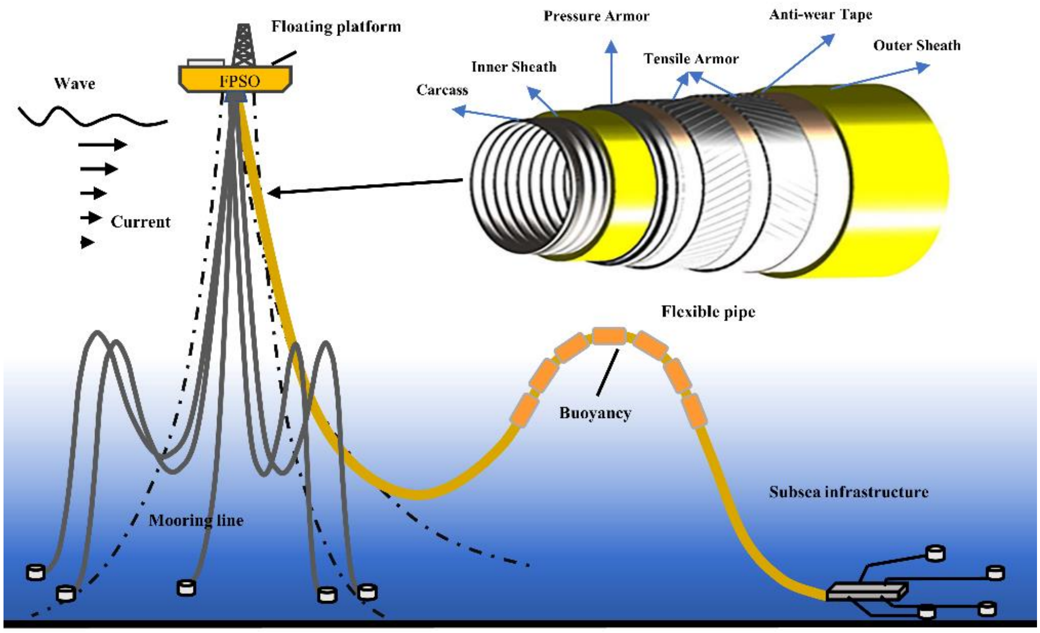

Figure 1. Floating production system and flexible pipe.

EF is the structural interface in the top connection area; only an anchorage system transfers all the axial stress from the flexible pipe body and the helically armored steel wire to the epoxy resin inside the end-fitting body (shown in Figure 2). Offshore operational experience has proven that the EF region is the weakest point of the flexible pipe system [4].

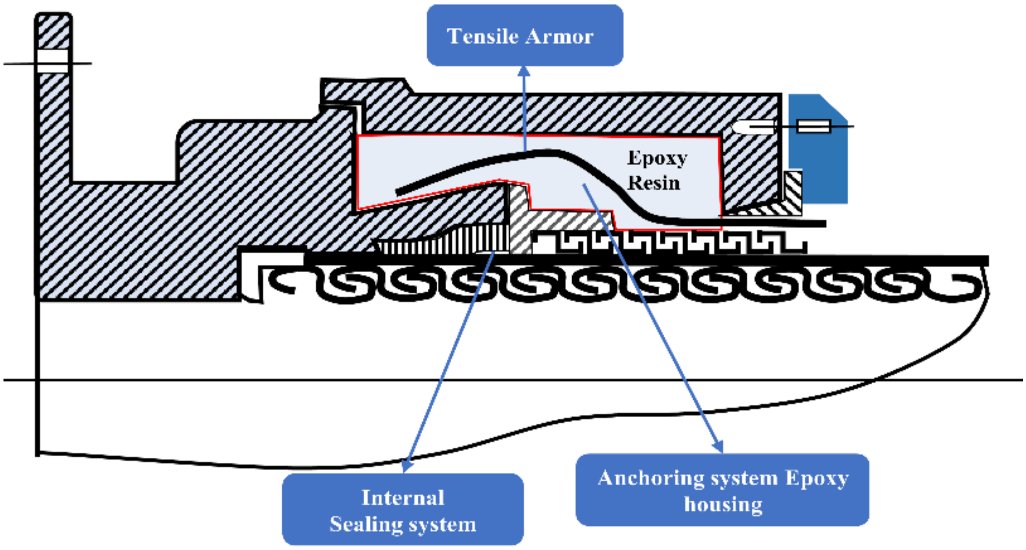

Figure 2. End fitting structure diagram.

The study of the tension behavior of flexible pipes has a long history, and numerous researchers have investigated the mechanical behavior of flexible pipes using analytical and numerical analysis and taking into account the deformation and slip of tensile armor under tension loads [5,6]. Furthermore, Yue et al. [7] carried out an experiment on a large scale to support the results of the numerical analysis. Dong et al. [8,9] investigated the impact of end fittings on the stress evaluation of tensile armor tendons in unbonded flexible pipes that were subjected to axial tension. However, the focus of this research was on the pipe body's capacity for deformation; the bearing capacity under extreme tension, particularly in the end fitting region, was neglected.

The fatigue failure of the tensile armor inside the end fitting has received extensive attention. Shen et al. [10] proposed a finite element (FE) model considering resin debonding and complex geometry to predict the stress characteristics of the tensile wire inside the end fitting. The results indicate that the highest stress measured within the EF is greater than any other position along the pipe's body. Simultaneously, he conducted several small-scale test samples to confirm the FE analysis model. Xaiver [11] regards the steel wire in the end fitting as the metal bar in prestressed concrete. He proposed a new anchorage model with a lower concentration and analyzed the stress of the tensile armor wire. Daflon [12] studied the adhesion between the resin and tensile armor wire by conducting the tensile test on the single tensile armor wire and complete end fitting. The shear stress results were between 7.5 and 14.8 MPa. According to the results of the test that was carried out in the 2.5″ pipe end fitting, the tensile armor wires that are located inside the end fitting are of critical significance to the structural integrity of the flexible riser. Bueno [13] predicted the stress concentration factor through a 3D FE model, where the stress–strain characteristics of armored steel wire inside the end fitting are better described. Then, he carried out a full-scale test to verify the results of the numerical analysis. Sousa et al. [14] proposed a 2D FE approach to estimate the stress of tensile armors inside end fittings, and they performed a parametric study to investigate the influence of three parameters on the stress state along the wire. These three parameters are the contact conditions between the resin and tensile wire, the stress level during the factory acceptance test (FAT), and the resin's elastic properties. The study indicates that the stress distribution along the wire may be significantly affected by these parameters. Campello et al. [15,16] designed a novel concept of flexible pipe end fitting that they called tensile armor foldless assembly, which assessed the stress distribution and fatigue performance considering the EF mounting process and operational loads and quantified this difference between a novel concept EF and a conventional EF, claiming that the maximum stress on the key segment of the wires lay inside and that EF was expected to be approximately 2.4 times higher than the outside. Anastasiadis et al. [17] developed a finite element model in order to investigate the stress concentration characteristics of the steel wire inside the end fitting while taking into account the impact of the assembly process. They also proposed a formula that provided a rough estimate of the maximum stress concentration factor based on a parametric study. Miyazaki et al. [18,19] applied a 3D finite element model to perform fatigue analysis. According to the findings of this study, the level of the stress concentration that was connected with the EF assembly and FAT had a substantial influence on the fatigue life of the flexible pipes. Torres et al. [20] conducted laboratory tests to investigate the characteristics of epoxy resin. By modifying the ratio of resin to hardener, the compressive and adhesive capabilities of the epoxy resin were enhanced. Mattedi [21] proposed the improvement of the epoxy for the anchorage system, with a focus on the mechanical and adhesive qualities, by adding multi-walled carbon nanotubes (MWCNTs) to the mixture. In order to analyze the system's sensitivity to the features of the epoxy, an analytical model for the anchorage mechanism was built and then evaluated by numerical analysis. After that, the morphology of the nanotubes and the homogeneity of the matrix were expert-analyzed to see how they correspond with the mechanical results.

However, the existing study on the structural analysis of end fitting focuses mostly on the stress analysis of the steel wire and lacks precise information on the failure behavior of the entire anchorage system under extreme tension loads. There are relatively few historical investigations in the area of debonding failure between the epoxy resin and the tensile armor steel wire. The majority of the literature focuses on stress distribution and fatigue damage along the tensile armor wire inside the EF. This research aims to improve the understanding of the progressive failure behavior of end fitting. This study focuses on the debonding failure behavior under the tensile load of the epoxy resin and armored steel wire anchorage system inside EF. A numerical analysis method was used to predict the end fitting debonding failure behavior, and a model test was carried out to investigate the EF connection failure process.

2. Materials and Methods

The progressive failure behavior of EF anchorage systems in flexible pipes was investigated using numerical methods in this work, and the results were verified by model tests. The research process (shown in Figure 3) can be classified into four distinct steps:

1. Consider the geometry and loading direction of the end fittings to simplify the three-dimensional helical arrangements.
2. Conduct a single-lap shear (SLS) test to determine the material properties of the epoxy resin inside the end fitting.
3. On the basis of the properties of the materials gathered in step 2, use a CZM-based numerical model to investigate the progressive failure behavior of the anchorage system under an axial tension load. The failure process is described in terms of the time-dependent evolution of damage parameters and stress along the steel wire.
4. Perform model tests and compare the acquired load–displacement curves to the numerical results in order to determine the validity of the numerical model developed in this research.

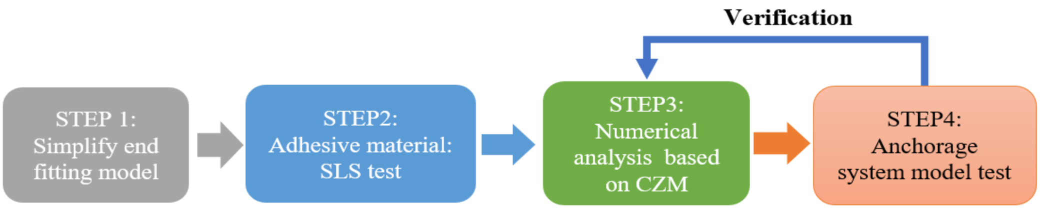

Figure 3. Research process flow diagram.

2.1. End Fitting Structure and Model Simplification

The end fitting is intended to prevent the pulling out of the tensile armor under dynamic and static service loads. Utilizing an embedded epoxy to secure the tensile armors of a flexible riser into the end fitting is a typical approach that gives excellent mechanical and chemical protection. To fulfill the requirements of the end fitting sealing system assembly and to improve the axial load capacity, the armor steel wire has a complicated geometric shape and is placed with a helical angle between 20 and 50 degrees.

It is recommended that the end fitting model is simplified due to the complexity of the internal structure and the limitations of the computational capacity. Because Campello et al. [4] pointed out that any axial stress operating on the flexible pipe is supposed to be distributed equally along all the pipe armor wires, the double-layer armor can be simplified to a single layer when taking into consideration the axial load. Recent papers by Shen et al. [16] represented the entire EF as a longitudinal slice, and the helical structure of the tension was ignored. This is in contrast to the representation of the complete EF as a slice. Referring to the common practice in the existing literature, this paper simplified the bearing of the 3D helical model into a 2D model (shown in Figure 4).

2.2. Single Lap Shear Test for Adhesive Material Properties

Practical engineering applied the single lap shear test (according to ASTM D4896 [22]) to acquire accurate material properties. In this article, a single-lap shear test was conducted using a tensile testing machine (experiment setup and sample dimension are shown in Figure 5a). In order to prevent the large deformation of the steel plate during the test, the steel plate is made of high-strength galvanized steel. First, use 100# sandpaper for surface sanding, use acetone solution to clean the surface, apply adhesive according to the design size, and apply pressure to ensure a strong bond. Cure at 120 °C for 6 h. Finally, leave it for 24 h before carrying out the experiment.

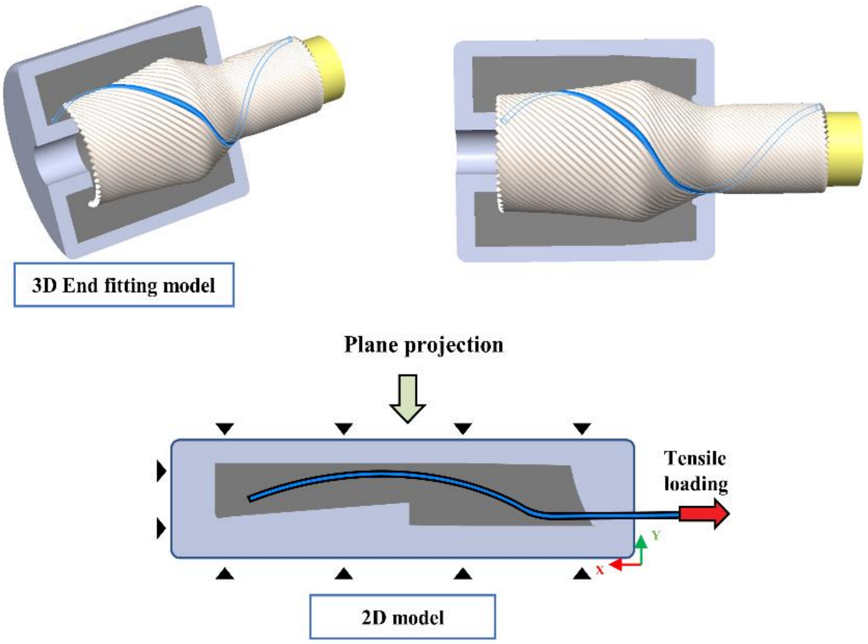

Figure 4. End fitting model and simplification.

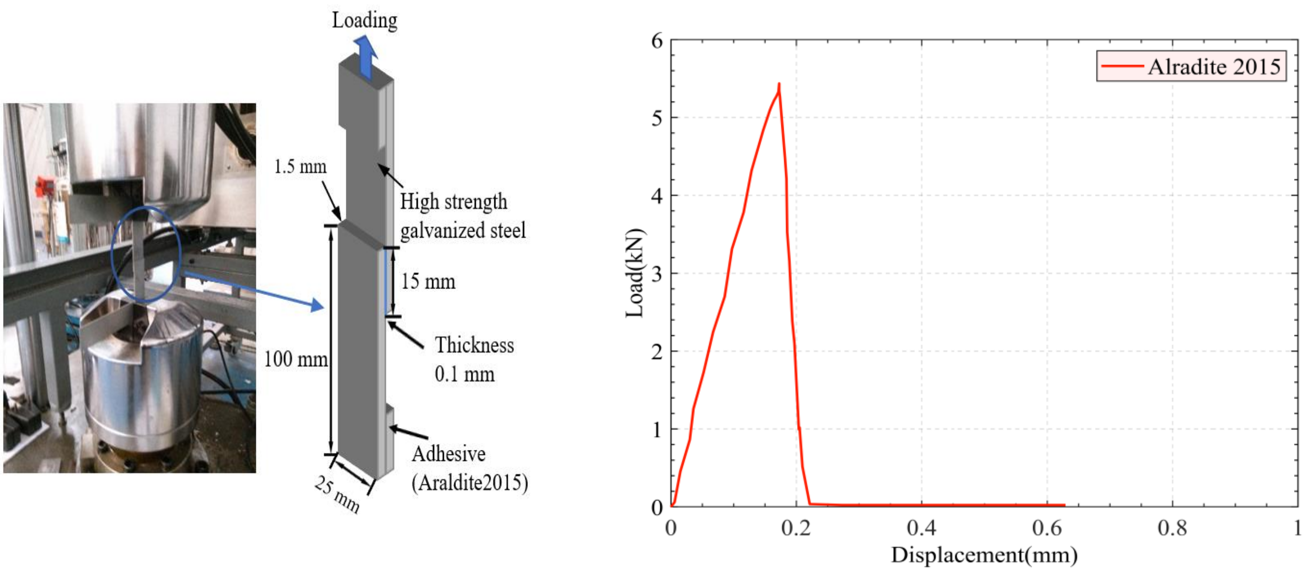

(**a**) (**b**)

Figure 5. Single-lap shear test; (**a**) Experiment setup and sample dimension (**b**) Load–displacement curve in SLP test.

The load–displacement curve is illustrated in Figure 5b. As can be seen, the load increases linearly until it reaches the point of maximum shear force, at which point failure occurs. The shear strength of Araldite 2015 is 15.3 MPa; other parameters that are required for the simulation are derived from Campilho et al. [23] (listed in Table 1).

Table 1. Properties of the adhesive Araldite 2015 for CZM modelling.

Stiffness (MPa)		Strength (MPa)		Separation Energy (N/mm)	
Elastic	Shear	normal	Tangential	I-crack	II-crack
1850	560	18.36	15.3	0.5041	0.7915

2.3. Finite Element Analysis Based on Cohesive Zone Model(CZM)

2.3.1. Cohesive Zone Model for Bonding Structure

The evaluation of interface debonding is based on the mechanics of elastic-plastic fracture, despite the fact that the theoretical method is often applied only to simple geometries under unidirectional stresses. However, the complicated fracture problems of practical engineering structures sometimes necessitate costly and time-consuming testing. When dealing with the issue of debonding failures, a multi-method that combines numerical analysis with restricted experimental verification can save time and has found widespread application.

The cohesive zone model (CZM) [24] and virtual crack closure technique (VCCT) [25] are the primary FEM methods used for interface fracture mechanics. The CZM approach can focus on interface debonding initiation and propagation; CZM approach can focus on interface debonding initiation and propagation, in addition to using mixed failure modes (as depicted in Figure 6a), while the VCCT method considers the failure of the composite immediately after the loss of adhesion and is mainly used for failure mode I. CZM is used to characterize the material constitutive relationship during the failure process in order to evaluate the progressive debonding failure behavior of a steel wire-resin anchorage system.

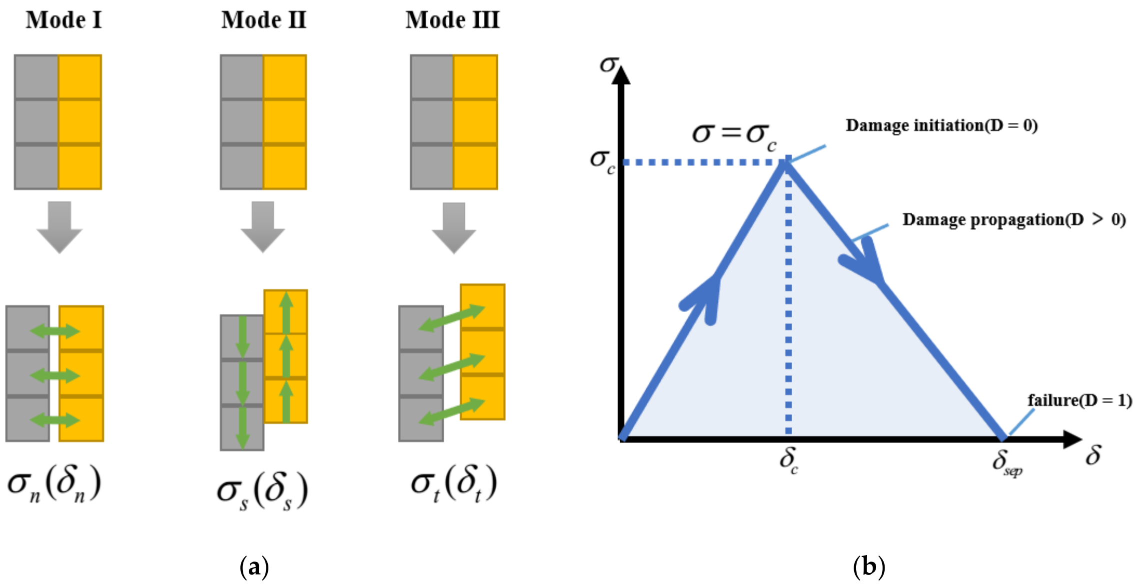

Figure 6. Cohesive zone damage; (**a**) Traction separations for different fracture modes; (**b**) Typical bilinear traction separation behavior.

CZM establishes the interface's material behavior from elastic deformation to damage accumulation and total debonding via a traction—separation relationship. The most common CZM behavior is the bilinear debonding law, as shown in Figure 6b. This paper focuses on the failure behavior under tensile loading. In the simplified model, the contact stress across the interface increases and reaches a maximum, declines, and is eventually compromised, leading to a complete debonding.

Figure 6b illustrates the behavior of the traction-separation law for a single fracture mechanism. If one fracture mode is acting alone, the crack is initiated at σ_c. When the bonding system is in the process of loading, the relative displacement of the contact surfaces results in contact stress in the cohesive zone. K is the ratio of contact stress to contact separation before the damage occurs. δ_c is the critical separation when the damage occurs. Then, the damage grows, and the interface stiffness decreases. When the maximum displacement δ_{sep} is reached, the contact surfaces are entirely separated. Equations (1) and (2) below are the governing equation for the bilinear cohesive zone model, which apply to all three separation failures in Figure 6a. The damage can be measured by the damage parameter D, which is defined by Equation (1):

$$D = \begin{cases} 0 & \delta \le \delta_c \\ \frac{\delta_{sep}(\delta - \delta_c)}{\delta(\delta_{sep} - \delta_c)} & \delta_c \le \delta \le \delta_{sep} \end{cases} \tag{1}$$

Govern equations for bilinear as Equation (2):

$$\sigma = \begin{cases} \frac{\delta}{\delta_c}\sigma_c & \delta \le \delta_c \\ (1 - D)\frac{\delta}{\delta_c}\sigma_c & \delta_c \le \delta \le \delta_{sep} \end{cases} \tag{2}$$

ABAQUS 2020 [26] was utilized to represent the cohesive zone in the interface debonding. To improve the calculation's accuracy, it is essential to input the accurate material parameters and select the appropriate failure criteria. In this article, the square stress criterion is employed to determine the initiation of the damage, whereas the Power law criterion is used to determine fracture failure.

2.3.2. Finite Element Model Setup

A finite element model of the tensile armor pull-out from the anchorage system was generated using the CZM approach. The model consists of three parts: outer casing, epoxy resin, and tensile armor steel wire. The end-fitting outer casing is set as a fixed support, the contact between the epoxy resin and tensile armor is set as a cohesive behavior, and the displacement load is applied to the end of the tensile armor to simulate the failure process of the anchorage model. The geometry is shown in Figure 7.

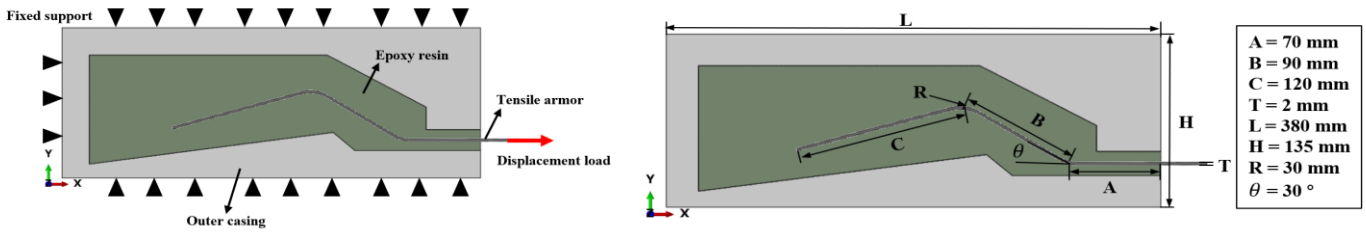

(a) (b)

Figure 7. FE Model; (**a**) Model and boundary condition (**b**) Model geometry.

The material and input parameters are summarized in Table 1. The contact behavior of the interface was modeled, as discussed in Section 2.3, using bilinear cohesive behavior. A displacement-controlled load of 8 mm was applied at the free end of the fiber. To investigate the failure behavior of a flexible pipe EF anchorage system, THE simplified finite element model of the anchorage system consists of three parts: the outer casing, the tensile armor, and the epoxy resin. To simplify the calculation process, the outer casing, which has very little deformation, is considered a linear elastic material (Young's modulus is 210 GPa). For the tensile armor, a bilinear hardening model is adopted, as follows. Young's modulus is 210 GPa, the yield strength is 235 MPa (yield strain is 0.01), and the ultimate strength is 400 MPa (failure strain is 0.23). The epoxy resin is considered to be an isotropic linear elastic material with Young's modulus of 3800 MPa.

The simplified model studied in this paper is comparable in size to a thin plate, and the structure's deformation and failure behavior is driven by an in-plane tensile load, which can be equivalent to a two-dimensional model. The load-bearing capacity of a 2D model is the result of per unit thickness and grows proportionally with plate thickness. Each component of the model uses the CPS4R element (4-node bilinear, reduced integration with hourglass control) to balance computational efficiency and precision, as is shown in Figure 8. Surface bonding is simulated by cohesive contact behavior, which implies that the failure of the cohesive bond is characterized by the increasing degradation of the cohesive stiffness caused by damage.

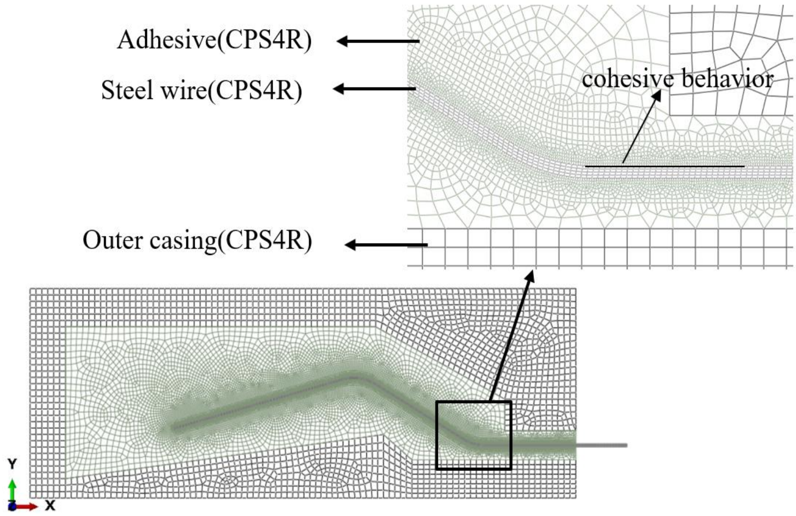

Figure 8. Mesh and element type of FE model.

2.4. Model Test of Anchorage System

The model test is employed to validate the results of the numerical analysis [27]; the test sample has the same dimensions as the numerical model. During the pull-out test, a tensile testing machine is used to apply a 10 mm displacement load (2 mm/min), and the pull-out force and displacement curve of the test is measured. The experiment is illustrated in Figure 9. In Section 3.1, the results are described in great detail.

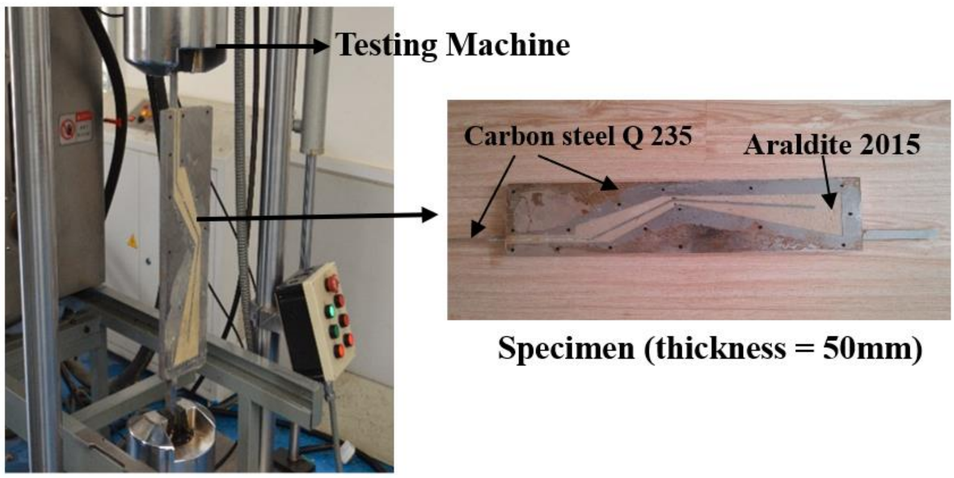

Figure 9. Experiment setup of model test.

3. Numerical and Experimental Results

This section contains a load–displacement curve from the FEM and an experiment to describe the progressive behavior of the end-fitting model through the evolution of the mises stress distribution along the steel wire orientation and the interface damage factor CSDMG during the loading process. Finally, the failure behavior of the anchorage systems with a different yield strength for steel wire and adhesive shear strength is investigated.

3.1. Load–Displacement Curve from FEM and Experiment

The results of the model test stated in Section 2.4 are shown in the figure below. For the anchorage system consisting of Q235 carbon steel (ys = 235MPa) and adhesive (Araldite 2015), an experiment and finite element analysis based on the cohesive zone model was performed.

The FEM and experimental results of the relationship between the tensile load and displacement of the flexible pipe end fitting anchorage system when subjected to an axial load are shown in Figure 10. It can be seen that the finite element approach has a matching growth trend to the load–displacement curve derived from the experimental results, indicating the finite element method's feasibility for predicting the anchorage system's debonding failure behavior.

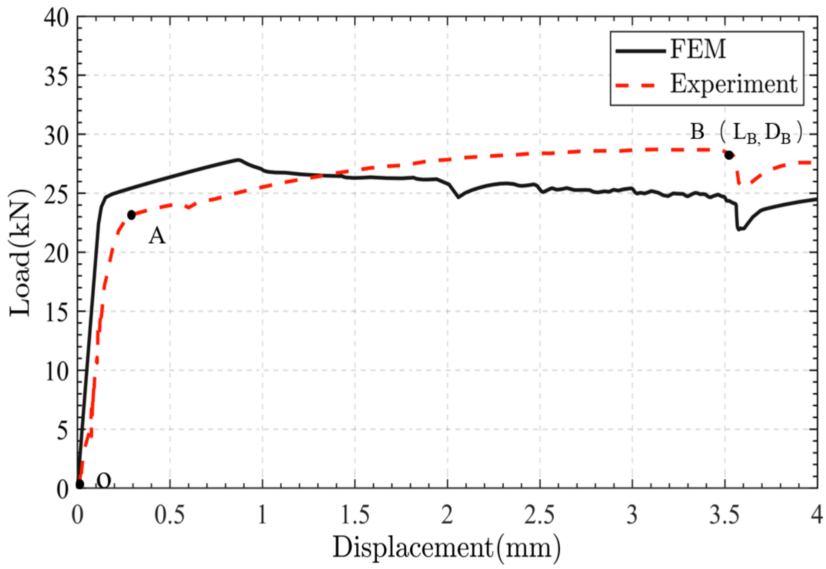

Figure 10. Load–displacement curve of the anchorage model.

A further observation of the load–displacement curve demonstrates that, along with the loading process, the tensile load first appears to grow rapidly from point O to point A due to the steel wire's elastic deformation. Additionally, after point A, the rate of expansion slows, and the tensile load plateaus; the change in the slope after point A may be due to the plastic deformation of the wire and the initiation of interface bonding damage. The top of the curve is located at point B, and from point A to point B, the damage expands rapidly while the wire undergoes plastic deformation. At point B, the anchorage system totally fails, and the load drops sharply after reaching this location. Point B's coordinate is (L_B, D_B). L_B is the failure load, which indicates the maximum bearing capacity of the anchorage system, and D_B is the failure displacement.

3.2. Stress Evolution of Steel Wire

Mise's stress in the tensile armor steel wire is a key indicator of the anchorage system's failure condition. By analyzing the evolution of the Mises stress throughout the length of the wire during the loading process, it is possible to better understand the failure mechanism of the EF anchorage system.

Figure 11a shows the entry point of the anchorage structure (x = 0) and the Mises stress distribution along the steel wire. Figure 11b illustrates the stress evolution of the wire from d1 to d7; the specific values for d1–d7 are shown in the Figure legend. From d1 to d3, the Mises stress along the steel wire decreases gradually due to the shearing effect of the adhesive, with the rate of decline likely being related to the adhesive's shear strength. From d4 to d5, when the steel wire Mises stress near the entry initially exceeds the yield strength, plastic deformation occurs, and the length of the yield section expands gradually toward the inside as the load increases. From d6 to d7, a stable plateau appears along the stress distribution of the wire, denoting that the shear effect disappears, the interface between the wire and the adhesive becomes debonded, and the stress distribution of the wire can indicate adhesive failure. The above-described stress evolution characteristics are generally consistent with the failure mechanism characterized by the load–displacement curve in Section 3.1.

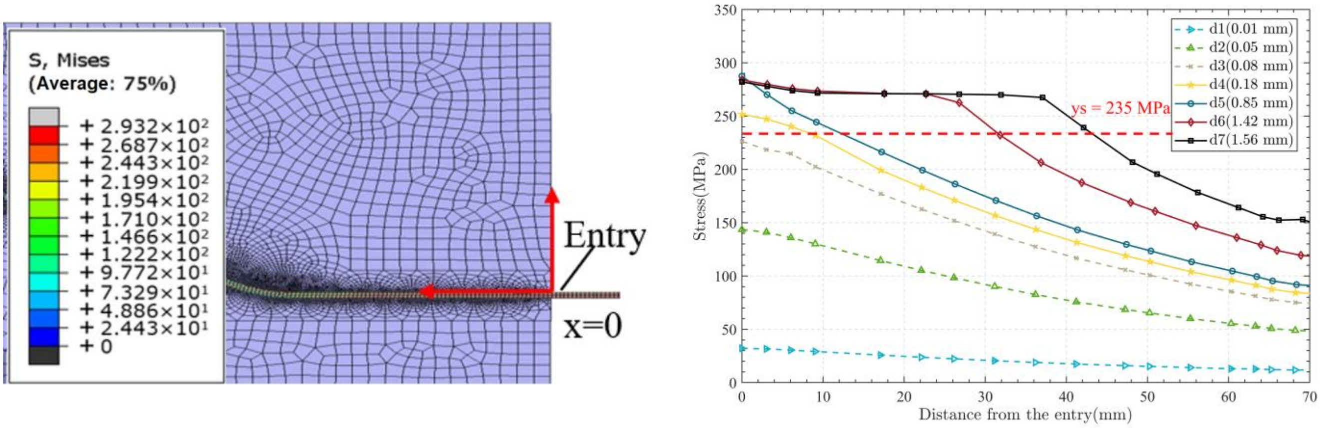

(**a**) (**b**)

Figure 11. Steel wire Mise stress distribution; (**a**) Zero position; (**b**) Stress distribution at different displacement.

3.3. Failure Process of Anchorages System

For the visualization of the debonding process of the flexible pipe end fitting anchorage model, the cohesive surface damage (CSDMG) parameter D is adopted in ABAQUS. CSDMG = 0 denotes the undamaged material, but CSDMG = 1 denotes the total material failure (no material stiffness) for the cohesive surface.

Figure 12 illustrates the progressive failure process of the EF anchorage system. The initial structure is not damaged during the loading procedure; this is known as the undamaged status. Currently, the CSDMG interface value is 0. With further loading, the wire gradually reaches its elastic limit, plastic deformation occurs, debonding initiation begins, the CSDMG = 1 position begins to appear, and the failure position begins at the entry point (x = 0). As the load grows, the inside gradually experiences damage. The axial shear stress dominates the surface and its debonding propagation process. Eventually, the structure appears to be totally debonded, and the damage parameter CSDMG of the whole straight section reaches 1. Although there are still internal twisted sections of wire in a bonded state, the failure of straight parts is unacceptable for the EF; therefore, this state is considered a structural failure.

When d = 0.85 mm, debonding starts at the connection position of the wire and the adhesive; debonding failure grows inside continuously with the loading process; and when d = 3.56 mm, total debonding happens in the straight section of the wire, when the tensile load reaches its peak.

3.4. Influencing Parameter Analysis

3.4.1. Different Steel Wire Yield Strength

The anchorage system consists of steel wire and epoxy resin, and the current API code primarily addresses the steel wire utilization factor when designing end fittings. This study shows that there are limitations in forecasting the structural failure behavior based on the linear elasticity of the steel wire and that it is advantageous to consider elastic plasticity in order to improve the load-bearing capacity of the anchorage system. Taking into account the elastic-plastic behavior of steel wires, this paper investigates the failure behavior of an anchorage system composed of four commonly used types of steel and the same epoxy resin adhesive (Araldite 2015). The material properties of different steels are shown in Table 2.

Table 2. Material properties of different steel material.

Material	Young's Modulus (GPa)	Yield Strength (MPa)	Ultimate Strength (MPa)
Steel A	210	235	400
Steel B	210	450	560
Steel C	210	800	950
Steel D	210	1200	1350

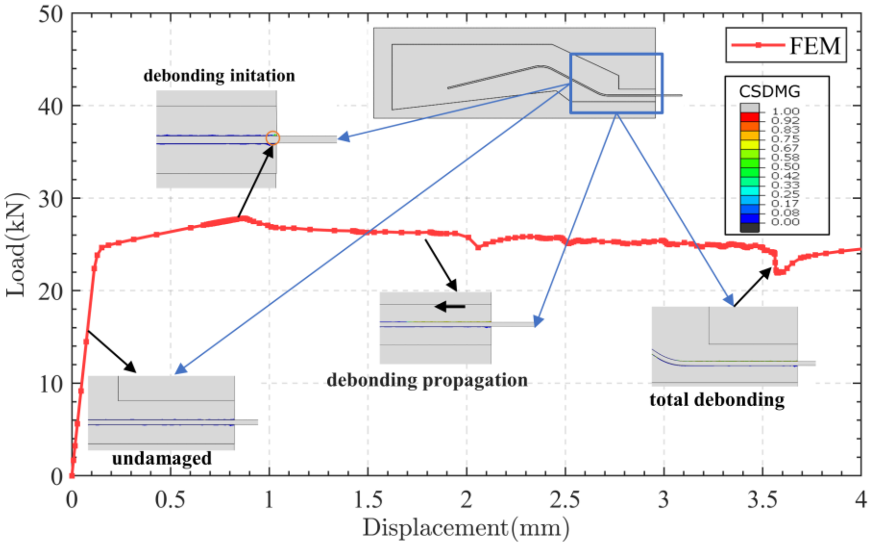

Figure 12. Failure process of the anchorage system.

The load–displacement curves of the anchorage system made of a variety of steel wire materials are illustrated in Figure 13. There are distinct differences between the load–displacement curves of different steel wire materials. As for Steel A and Steel B, which are carbon steel with low yield strength, the curves demonstrate three stages from the increase to plateau and decline where the anchorage system yields and generates plastic deformation before interfacial debonding leads to structural damage. In this case, enhancing the yield strength of the tensile armor wire can further improve its structural load capacity. The load–displacement for Steel C and D have higher yield strength and have only two stages, rising and falling, without significant plastic deformation; in this situation, bond failure is the dominant cause of failure. The load–displacement curves are remarkably similar for different yield-strength steel wires; increasing the yield strength (ys) of the wire does not increase the load-bearing capacity of the anchorage system.

3.4.2. Different Adhesive Shear Strength

The adhesive material's properties also have an essential influence on the load-bearing capacity of the anchorage structure. This paper focuses on the failure behavior of pipe end fittings under tensile loading; as the tensile load is parallel to the wire direction, the shear strength of the wire-epoxy bond interface is the crucial variable that dominates the debonding of the interface. Comparing shear strengths, the results obtained for nominal strengths and stiffnesses are not significantly different. Therefore, in this study, which focuses on the effect of adhesive shear strength, the load-bearing capacity of anchoring systems consisting of various wire materials and epoxy resins with different shear strengths was investigated. The shear strength properties of different adhesives are listed in Table 3.

Table 3. Shear strength of different adhesives.

Material	Interface Shear Strength (MPa)
Adhesive A	15.3
Adhesive B	18.36
Adhesive C	19.89
Adhesive D	21.42

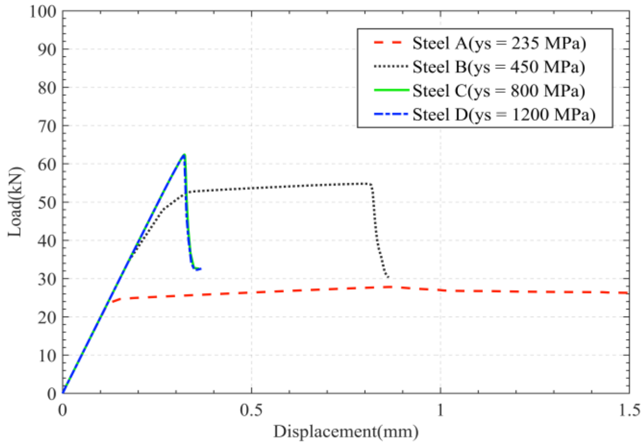

Figure 13. The load–displacement of the anchorage system consists of different steel wire.

Figure 14a illustrates the calculated load–displacement curves of 450 MPa steel wire with various shear strength (SS) adhesives. The data show that when the interface shear strength grows, the structural load-bearing capacity remains constant while the failure displacement continues to increase. The increase in the load-bearing capacity driven by the rise in shear strength is constrained because wire yielding occurs prior to structural debonding in this situation. Figure 14b–d, respectively, show the load–displacement curves of an anchorage system that is composed of various yield strengths of 800 MPa, 1200 MPa, and 1300 MPa. In this situation, plastic deformation has not yet occurred when interfacial debonding takes place, and the interfacial debonding that occurs as a result of the insufficient adhesive shear strength is the predominant factor that contributes to failure.

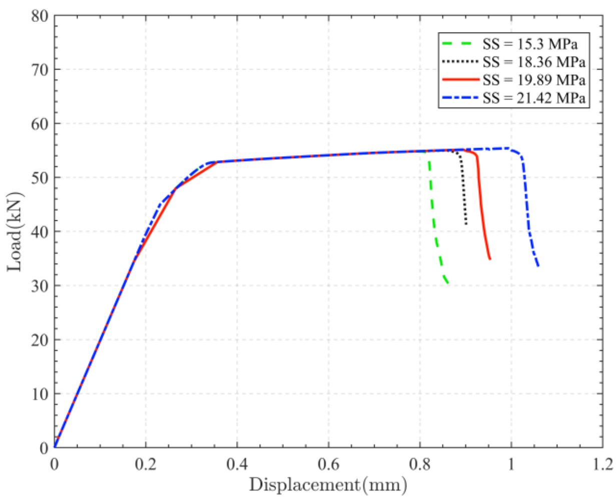

(**a**)

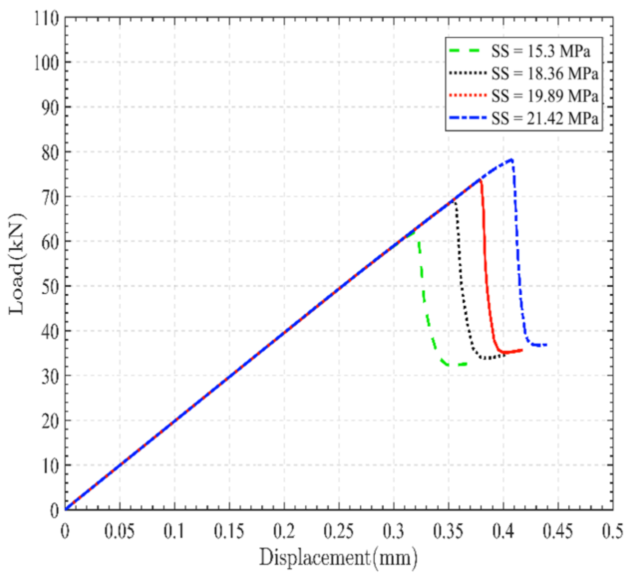

(**b**)

Figure 14. *Cont.*

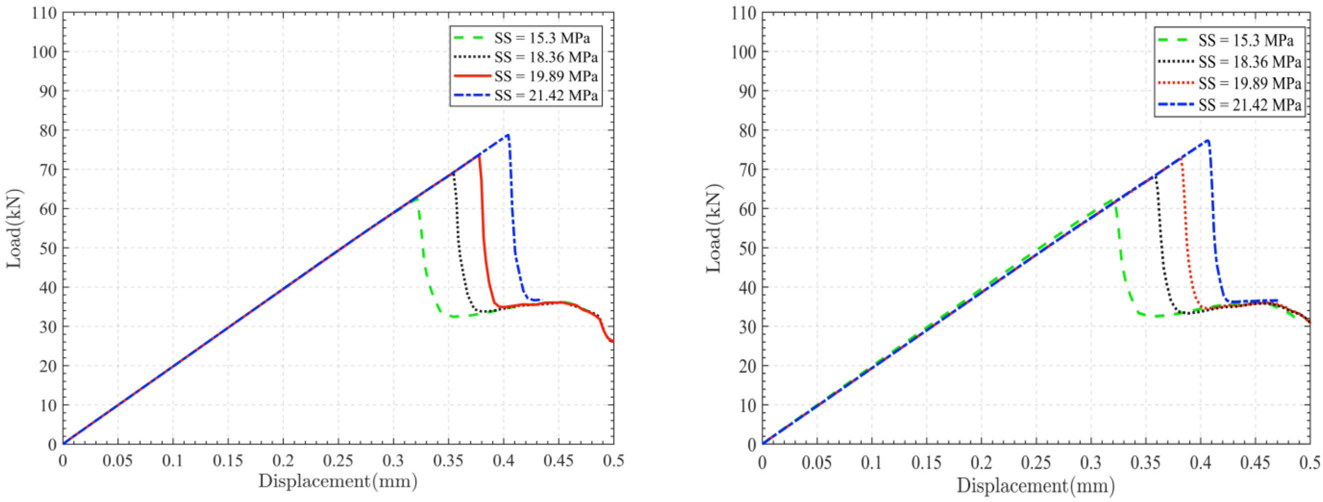

(**c**) (**d**)

Figure 14. Load–displacement of different materials; (**a**) ys = 450 MPa; (**b**) ys = 800 MPa; (**c**) ys = 1200 MPa; (**d**) ys = 1300 MPa.

4. Discussion

There are three failure modes for similar bonding systems according to the composite failure theory: wire failure, interface debonding, and epoxy resin failure. Due to the protection provided by the EF outer casing, the breakdown of the epoxy resin is less likely to occur. Therefore, wire plastic fracture and interface debonding are employed as the primary failure modes of flexible pipe EF. This paper discusses the failure modes of the flexible pipe end fittings and the factors affecting the structural load-bearing capacity based on the previous calculation results.

4.1. Progressive Failure Behavior

The relative magnitude of the wire yield strength compared to the interfacial shear strength of the epoxy resin causes significant differences in the failure behavior of the anchorage system.

The load–displacement curve shows three stages of growth, plateau, and decline, which indicates that the failure of the structure can be divided into three stages: elastic bonding, debonding propagation, and the final failure stage. The failure of the steel wires occurs prior to the debonding of the interface in the anchorage system that is composed of low-yield strength steel wires. The elastic bonding stage is characterized by a linear relationship between the load and displacement; the shape of this curve is controlled by the elastic modulus and yield strength of the steel wire. As Young's modulus increases, the slope of the curve increases, and the maximum load rise as the yield strength increases. The peak load is not significantly increased by the increase in shear strength since the wire undergoes plastic deformation throughout the debonding extension phase. Additionally, the plastic deformation increases the failure displacement.

The structural failure process for anchorage systems made of high-yield strength steel wires typically does not include plastic deformation. The load–displacement curve has only two stages; the failure of the bonding interface is the predominant failure mode, and the interfacial shear strength of the wire and epoxy is the most crucial factor governing the peak load.

4.2. Influence Parameter on Load-Bearing Capacity

The failure displacement of the anchorage system with various material combinations is summarized in Figure 15. The three-stage failure is observed to have a higher failure displacement than the two-stage failure due to plastic deformation. Comparing the failure displacement of steels C, D, and E indicates that the yield strength has no effect on the failure displacement; however, an increase in the shear strength at the bonding interface can significantly increase the failure load and displacement. For steel C, failure displacement rises by 9%, 17%, and 23% for 20%, 30%, and 40%, and increases in epoxy resin shear strength, respectively. The absence of an impact of different steel wire strengths on the percentage increase further confirms the notion that interfacial bonding failure predominates in a two-stage failure.

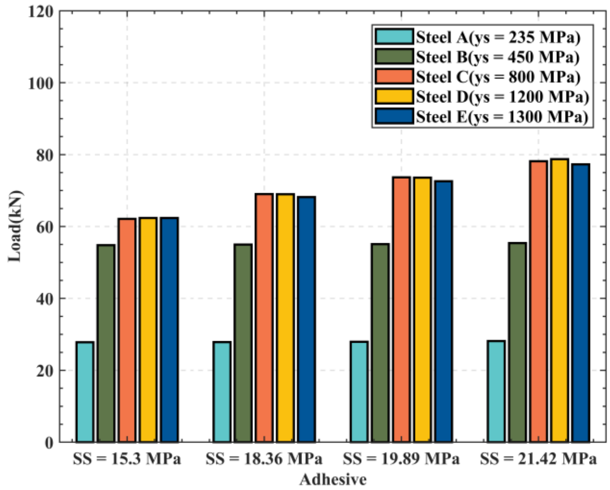

Figure 15. Failure displacement of different anchorage systems.

Figure 16 illustrates the failure loads for different material combinations. Two-stage failure has been found to have a larger failure load than three-stage failure. For steels A and B, an increase in the interfacial shear strength does not significantly improve the structural load-bearing capacity. Nevertheless, increases in the shear strength of 20%, 30%, and 40% might enhance structural failure loads by 11%, 16%, and 22%, respectively, for steels C, D, and E.

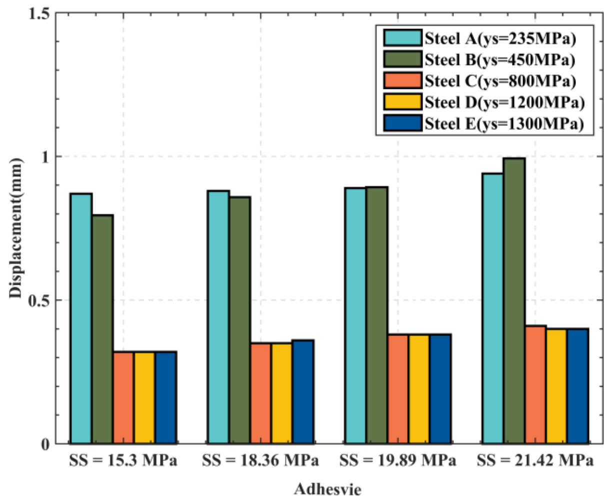

Figure 16. Failure load of different anchorage system.

5. Conclusions

Deep-water oil and gas development is limited by the load-bearing capacity of the anchorage system in flexible pipe end fittings. The existing literature emphasizes the failure behavior of steel wires under static and dynamic axial loads but rarely considers the debonding behavior between steel wires and resin. In this paper, we conducted a numerical study on the progressive failure behavior of the anchorage system in end fittings under the axial tension brought by the self-weight of the pipe using the ABAQUS software. We then discussed the influencing factors that affect the load-bearing capacity and failure behavior of the anchorage. According to the results of this research, the following conclusions and suggestions can be made:

1. The finite element method based on the cohesive zone model can effectively simulate the mechanical behavior of the anchorage system under axial loading. The load–displacement curve obtained from the numerical simulation has similar growth trends compared with the experimental result.
2. Further investigation of the load–displacement curve of the anchorage system under axial load leads to the conclusion that the failure behavior of flexible pipe end fittings significantly depends on the material selection of the anchorage system, with two and three stages.
3. Two-stage failure behavior is common in end fittings consisting of high-strength tensile armor steel wire, which is characterized by no plastic deformation in the steel wire, only a linear bonding, and debonding stage, in the load–displacement curve. Interfacial debonding is the predominant failure mode; hence, increasing the interfacial shear strength of the epoxy resin adhesive can significantly enhance the load-bearing capacity of the structure.
4. Three-stage failure behavior is common in end fittings consisting of low-strength tensile armor wire, which is characterized by the obvious plastic deformation of the wire and three stages of the load–displacement curve: elastic bonding stage, debonding stage, and the final failure stage. Steel wire failure is the dominant failure mode rather than interface debonding. Improving the yield strength of the wire can effectively increase the structural load-bearing capacity; however, increasing the interface shear strength of the epoxy resin adhesive has little or no effect on the failure load but can increase the failure displacement.

In conclusion, this paper investigates the failure behavior of the flexible pipe end fitting anchorage system using numerical and experimental methods and then analyzes the significant influence of the material selection on failure behavior by introducing the cohesive zone model to evaluate the interfacial debonding process between the tensile armor steel wire and epoxy resin during the loading process. This study's findings about the progressive failure behavior of end fitting anchorage systems can be applied to the design and development of anchorage systems for ultra-deep water flexible pipe end fittings.

Author Contributions: Conceptualization, T.Z.; Data curation, T.Z. and S.W. (Shanghua Wu); Formal analysis, T.Z. and J.C.; Funding acquisition, J.Y.; Investigation, T.Z.; Methodology, T.Z. and H.L.; Project administration, Q.L. and Q.Y.; Resources, J.C. and J.Y.; Supervision, Q.Y.; Validation, T.Z. and S.W. (Shichao Wang); Visualization, T.Z. and S.W. (Shanghua Wu); Writing—original draft, T.Z.; Writing—review and editing, Q.L. and H.L. All authors have read and agreed to the published version of the manuscript.

Funding: This research was financially supported by the National Natural Science Foundation of China (Nos. U1906233, 52201395, 52201312), Natural Science Foundation of Jiangsu Province (BK20201198), Fundamental Research Funds for the Central Universities (No. 82232013), and Research and Development Projects in Key Areas of Guangdong Province (No. 2020B1111040002).

Institutional Review Board Statement: Not applicable.

Informed Consent Statement: Not applicable.

Data Availability Statement: Not applicable.

Acknowledgments: The authors highly appreciate the financial support provided by the Natural Science Foundation. We would like to acknowledge the reviewers and the editor for their valuable comments and suggestions.

Conflicts of Interest: The authors declare no conflict of interest.

References

1. Bruschi, R.; Vitali, L.; Marchionni, L.; Parrella, A.; Mancini, A. Pipe technology and installation equipment for frontier deep water projects. *Ocean Eng.* **2015**, *108*, 369–392. [CrossRef]
2. API. *Recommended Practice for Flexible Pipe*, 5th ed.; American Petroleum Institute: Washington, DC, USA, 2014.
3. Xiong, H.; Bai, Y.; Fang, Q.; Tang, G. Analysis on the ultimate bearing capacity of plastic pipe reinforced by cross-helically winding steel wires under internal pressure. *Ships Offshore Struc.* **2018**, *13*, 264–272. [CrossRef]
4. Campello, G.C.; de Sousa, J.R.M.; Vardaro, E. An Analytical Approach to Predict the Fatigue Life of Flexible Pipes Inside End Fittings. In Proceedings of the Offshore Technology Conference, Houston, TX, USA, 2–5 May 2016.
5. Troels, V.L.; Egil, G.; Steen, K.; Kristian, G.; Anders, L.; Christian, B. Tension-bending analysis of flexible pipe by a repeated unit cell finite element model. *Mar. Struct.* **2019**, *64*, 401–420.
6. Lu, H.; Murilo, A.V.; Marcelo, C. Alternative analytical and finite element models for unbonded flexible pipes under axisymmetric loads. *Ocean Eng.* **2021**, *225*, 108766. [CrossRef]
7. Yue, Q.; Lu, Q.; Yan, J.; Zheng, J.; Palmer, A. Tension behavior prediction of flexible pipelines in shallow water. *Ocean Eng.* **2013**, *58*, 201–207. [CrossRef]
8. Dong, L.; Zhang, Q.; Huang, Y.; Liu, G. Slip and stress of tensile armors in unbonded flexible pipes close to end fitting considering an exponentially decaying curvature distribution. *Mar. Struct.* **2017**, *51*, 110–133. [CrossRef]
9. Dong, L.; Zhang, Q.; Huang, Y.; Liu, G.; Li, Z. End Fitting Effect on Stress Evaluation of Tensile Armor Tendons in Unbonded Flexible Pipes Under Axial Tension. *J. Offshore Mech. Arct.* **2018**, *140*, 51701. [CrossRef]
10. Shen, Y.; Ma, F.; Tan, Z.; Sheldrake, T. Development of the End Fitting Tensile Wires Fatigue Analysis Model: Sample Tests and Validation in an Unbonded Flexible Pipe. In Proceedings of the Offshore Technology Conference, Houston, TX, USA, 5–8 May 2008.
11. Xavier, F. Avaliação da Vida em Fadiga de um Novo Modelo de Terminal Conector para Dutos Flexíveis. Ph.D. Thesis, Universidade Federal do Rio Grande do Sul, Porto Alegre, Brazil, 2009. (In Brazilian Portuguese).
12. Daflon, M.B. Estudo de Aderência de Arames de Armadura de Tração em Conectores de Dutos Flexíveis. Master's Thesis, Universidade do Estado do Rio de Janeiro, Rio de Janeiro, Brazil, 2010. (In Brazilian Portuguese).
13. Bueno, A.F.B. De Tração de Riser Fleixível Durante Ensaios Axiais de Tração E Fadiga, Avaliação Das Armaduras. Master's Thesis, Universidade Federal do Rio Grande do Sul, Porto Alegre, Brazil, 2010. (In Brazilian Portuguese).
14. de Sousa, J.R.M.; Campello, G.C.; Bertoni, F.; Ellwanger, G.B. A FE Model to Predict the Stress Concentration Factors in the Tensile Armor Wires of Flexible Pipes Inside End Fittings. In Proceedings of the ASME 2013 32nd International Conference on Ocean, Offshore and Arctic Engineering, Nantes, France, 9–14 June 2013.
15. Campello, G.; Bertoni, F.; de Sousa, J.R.M.; Carpigiani, M.; Vardaro, E.; Mudry, G. A Novel Concept of Flexible Pipe End Fitting: Tensile Armor Foldless Assembly. In Proceedings of the ASME 2012 31st International Conference on Ocean, Offshore and Arctic Engineering, Rio de Janeiro, Rio de Janeiro, Brazil, 1–6 July 2012.
16. CAMPELLO, G.C. Metodologia de Projeto para o Sistema de Ancoragem de Conectores de Dutos Flexíveis e Proposição de Nova Tecnologia. Ph.D. Thesis, Universidade Federal do Rio de Janeiro, Rio de Janeiro, Brazil, 2014. (In Brazilian Portuguese).
17. Anastasiadis, P.S.; Theotokoglou, E.E.; Michailides, C. Numerical analysis of stress concentration factors on tensile armour wires inside the end-fitting of an axially tensed unbonded flexible pipe. *J. Struct. Integr. Maint.* **2020**, *5*, 72–86. [CrossRef]
18. Miyazaki, M.N.R. Stress Analysis of a Flexible Pipe Tensile Armor Wire during and after the End-Fitting Mounting. Ph.D. Thesis, Universidade Federal do Rio de Janeiro, Rio de Janeiro, Brazil, 2015.
19. Miyazaki, M.N.R.; de Sousa, J.R.M.; Ellwanger, G.B.; Da Silva, V.R. A Three-Dimensional FE Approach for the Fatigue Analysis of Flexible Pipes Tensile Armors Inside End Fittings. In Proceedings of the ASME 2020 39th International Conference on Ocean, Offshore and Arctic Engineering, Online, 3–7 August 2020.
20. Torres, R.N.; Tanaka, R.L.; Morini, R.G.; Otte Filho, O.O.; Vilela, T. Flexible Pipe Anchoring System: Resin Ratio Effects on Mechanical Properties. In Proceedings of the ASME 2015 34th International Conference on Ocean, Offshore and Arctic Engineering, St. John's, NL, Canada, 31 May–5 June 2015.
21. Mattedi, R.P. A Toughened Composite for Improving the Anchoring of Composite Tensile Armors of Flexible Risers. Ph.D. Thesis, Universidade Federal do Rio de Janeiro, Rio de Janeiro, Brazil, 2019.
22. *D4896-2001(2016)*; Standard Guide for Use of Adhesive-Bonded Single Lap-Joint Specimen Test Results. American Society for Testing and Materials: West Conshohocken, PA, USA, 2016.
23. Campilho, R.D.S.G.; Banea, M.D.; Neto, J.A.B.P.; da Silva, L.F.M. Modelling of Single-Lap Joints Using Cohesive Zone Models: Effect of the Cohesive Parameters on the Output of the Simulations. *J. Adhes.* **2012**, *88*, 513–533. [CrossRef]
24. Liu, X.; Jiang, J.; Wang, G.; Wang, J.; Xu, R. Debonding analysis of curved RC beams externally bonded with FRP plates using CZM. *Eng Struct.* **2020**, *205*, 110103. [CrossRef]
25. Senthil, K.; Arockiarajan, A.; Palaninathan, R. Numerical study on the onset of initiation of debond growth in adhesively bonded composite joints. *Int. J. Adhes. Adhes.* **2018**, *84*, 202–219. [CrossRef]

26. ABAQUS. *ABAQUS User's Manual; Dssault Systems*; ABAQUS: Paris, France, 2020.
27. Shang, D. Investigation on Adhesion of Unbonded Flexible Pipe End Fitting. Master's Thesis, Dalian University of Technology, Dalian, China, 2015. (In Chinese).